

Sue Ellen Haupt^{1,2}, Frank J. Zajaczkowski², Kerrie J. Schmehl²

¹National Center for Atmospheric Research, Boulder, Colorado

²The Pennsylvania State University, University Park, Pennsylvania

1. INTRODUCTION

Understanding the details of locale-specific flow in the atmospheric boundary layer (ABL) is critical to both siting wind power plants and to making short term predictions of wind variability. However, since atmospheric motion is described by nonlinear dissipative dynamical systems it is sensitive to initial and boundary conditions. Therefore, most practical approaches to modeling involve both ensemble averaging in the model formulation and parameterizing subgrid scale processes with a stochastic formulation. This approach results in an average flow with superimposed fluctuating flow. Modern time dependent Reynolds Averaged Navier Stokes (RANS) models operate this way. This approach produces an inherent mismatch between the wind field realization that occurs and the ensemble average calculation that is computed. This mismatch could lead to poor forecasts for situations where it is imperative to mimic the specific realization.

Our previous examples with simple models performed in the context of atmospheric transport and dispersion showed some success at using data assimilation to 1) identify the characteristics of the realization that is occurring and 2) use field observation data to back-calculate better flow modeling variables to match that realization (Haupt et al. 2009, Beyer-Lout 2007).

This current effort seeks to predict details of fine-scale motion that includes the impact of local terrain, heating information, land use processes, and input from a mesoscale numerical weather prediction model. The challenge is to assimilate such information into a standard computational fluid dynamics (CFD) model. Such an effort requires new assimilation techniques that merge profiles at several locations as computed by the mesoscale model into the CFD simulation without double counting the subgrid scale motions and that is smooth enough to prevent spurious gravity wave generation.

This new assimilation technique is tested in complex terrain near Rock Springs, PA with computed wind profiles input from fine resolution runs of the Weather Research Forecast (WRF) model run at Penn State. Section 2 describes the site. The mesoscale model as well as the CFD model are described in section 3. Section 4 also discusses the assimilation procedure. Section 5 gives some preliminary results while section 6 summarizes and discusses prospects for future work.

2. CASE DESCRIPTION

Our approach to testing our combined mesoscale and CFD modeling techniques is to construct case studies in an easily accessible site with meteorological monitoring on-site. The locale selected is thus the Rock Springs test site in central Pennsylvania nearby State College. The site is owned by The Pennsylvania State University and is instrumented with several meteorological towers that measure environmental fluxes in addition to wind and temperature variables at several different heights at several locations. The mountainous terrain is representative of locales that are frequently chosen to site wind power plants in central and western Pennsylvania. The terrain includes parallel mountain ridges that could be ideal for wind turbines. The ridges are separated by valleys well known for their agricultural value. In addition, our colleagues in the Meteorology Department at Penn State produce twice daily fine-resolution runs of WRF with nested domains of this region as discussed in section 3.1 below. The topography of this Central Pennsylvania region is depicted in Figure 1. The mountain ridges are oriented Southwest to Northeast and separated by broad valleys.

The initial case day chosen for initial analysis is a cold winter pattern on New Year's Eve Day of 2008 (model initialized at 0000UTC on December 31, 2008). The specific time for the CFD simulation is 2100UTC (1600 EST) on December 31. A cold front had just passed through the region leaving a pool of very cold Arctic air behind.

*Corresponding author address: Sue Ellen Haupt, Research Applications Laboratory, National Center for Atmospheric Research, Boulder, CO 80301; e-mail: haupt@ucar.edu

Temperatures sunk to about -10°C and surface winds were moderate (around 10 m/s) from the northwest, which is roughly perpendicular to the line of the mountain ridges, making for an interesting flow pattern at Rock Springs.

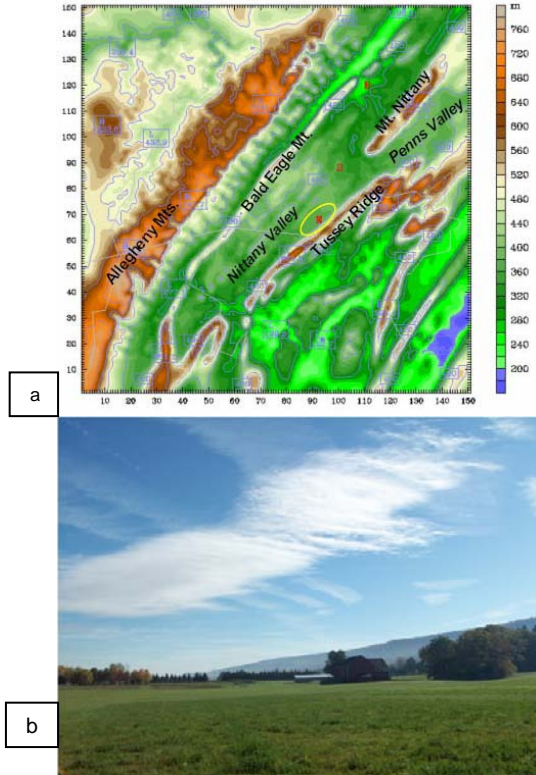


Figure 1. a. Topography of the region surrounding the Rock Springs site. The oval indicates the local observation network. b. Photograph of the local topography.

3. THE MODELING PROCESS

3.1 The WRF Model Setup

Fine-scale Numerical Weather Prediction (NWP) is used here to provide initial and boundary conditions for the CFD calculations. The mesoscale model runs use version 2.2.1 of the Advanced Research WRF (ARW) model (Skamarock et al. 2005). The model uses a third order scheme for vertical convection, fifth order finite differencing for the horizontal advection scheme, and third order Runge Kutta time integration. These schemes optimize the accuracy of small scale waves (Wicker and Skamarock 2002), which are important for correctly modeling fine-scale flow in complex terrain.

The five nested grid WRF-ARW configuration used here has resolutions of 36 km, 12 km, 4 km, 1.33 km, and 444 m (see Figure 2). The finest grid

is centered over Rock Springs, PA. The one-way nest interfaces from the coarser to the finer grids. There are 43 vertical layers for the finest horizontal mesh, with spacing concentrated near the surface with five layers representing the lowest 10 m as shown in Figure 3. This fine spacing is appropriate for the neutrally stable conditions observed on the case day. This configuration is initialized twice daily by the Stauffer research team at Penn State (<http://www.meteo.psu.edu/~wrf/rf/>). Four Dimensional Data Assimilation (FDDA) incorporates observations into the outer grids (see Stauffer et al. 2008).

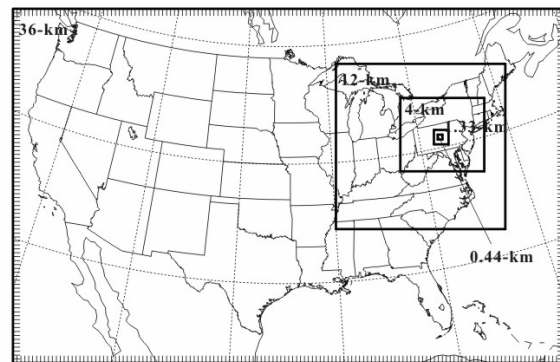


Figure 2. Nested grid configuration for model runs of the WRF-ARW model for studying atmospheric boundary layers in central PA.

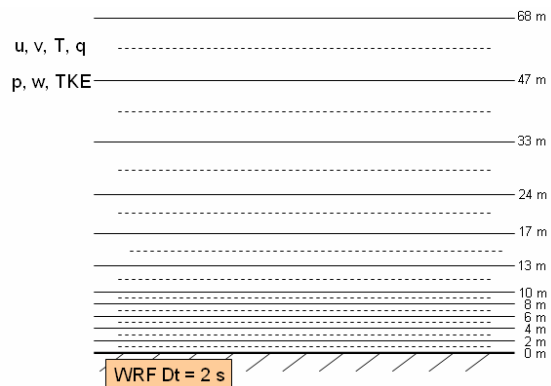


Figure 3. Vertical grid configuration for the lowest 70 m above ground level for the finest nest of the WRF-ARW runs.

3.2 Application of the Acusolve CFD Model

The goal of this effort is to assimilate the finest grid information from WRF-ARW into a high fidelity CFD simulation. This process is accomplished in two ways. First, the wind profiles computed by WRF are used as the inflow conditions for the CFD model. Second, profiles of the temporally and spatially varying flow field can be assimilated

to the CFD model at the correct time intervals at each of the WRF grid points.

The CFD simulations are done using the flow solver, AcuSolve (<http://www.acusim.com/>) from ACUSIM, Inc. AcuSolve uses a Galerkin/least squares finite-element flow method that is second-order accurate in space and time (Lyons et al. 2009). The code is capable of using a broad array of boundary conditions and includes data monitoring and data extraction tools. It is robust and accurate for application of both its RANS and Large Eddy Simulation (LES) modes. For this project, we use the RANS capability. AcuSolve can be used for modeling fine-scale details of flow around objects, including horseshoe vortices and separation and reattachment (Wilson et al. 2009) as well as the lee effects from upstream buildings (Long et al. 2009).

The domain modeled for Rock Springs has dimensions of 2.6 km x 2.0 km in the horizontal and is 1 km deep. The grid is composed of hexahedral elements and constructed using Gridgen, from Pointwise, Inc. Figure 4a shows the inner 444 m WRF domain with the inner AcuSolve domain marked. Figure 4b is a blowup of the terrain for the CFD mesh. The velocity profile plane that serves as the inflow boundary for the AcuSolve model is evident in that figure.

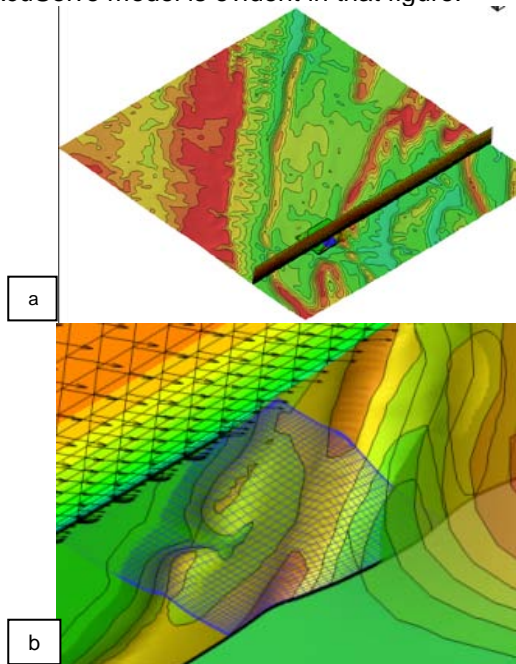


Figure 4. a) WRF 444 m domain with box over the Rock Springs Acusolve site b) blow-up displaying the Acusolve domain and the WRF determined inflow plane.

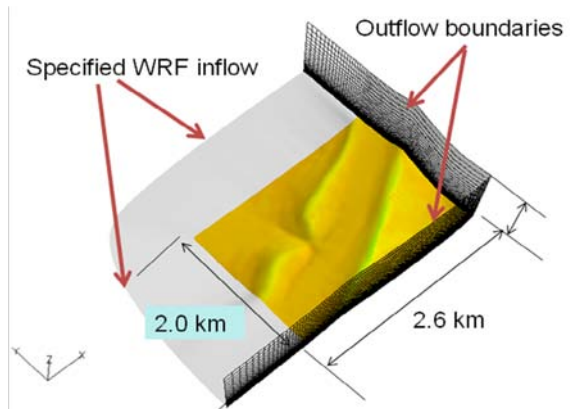


Figure 5. Boundary conditions for the computational domain.

The model applies no slip boundary conditions at the surface, inflow conditions from the WRF 444 m grid on the north and west sides, and outflow conditions on the east, south, and top boundaries. In order to avoid pressure field anomalies at the inflow, the domain has been modified to include a constant elevation “fetch” areas on the north and west sides of the domain as displayed in Figure 5.

4. ASSIMILATION

We incorporate the WRF mesoscale model data into the AcuSolve CFD simulation in two ways. First, we apply inflow conditions determined by WRF. Second, we directly assimilate at interior points by adding a body force model to AcuSolve. Both approaches are described and demonstrated below.

4.1 Inflow Modeling

Inflow conditions are compared using two different methods. In the control experiment, a constant inflow of 10 m/s is used everywhere. In the second experiment, we input a spatially varying inflow, both vertically and horizontally, from the WRF 444 m grid as shown in Figures 4 and 5.

Figure 6 shows the impact of including a velocity profile as computed by WRF as an inflow condition to Acusolve. Figure 6a indicated that if no inflow condition is provided (that is, a constant inflow is used), AcuSolve is not able to spin up a realistic velocity profile, even after a substantial integration time on a sufficiently fine grid. In contrast, when initialized with the velocity profile computed by the fine mesh of WRF (Figure 6b), the resulting velocity profile is realistic.

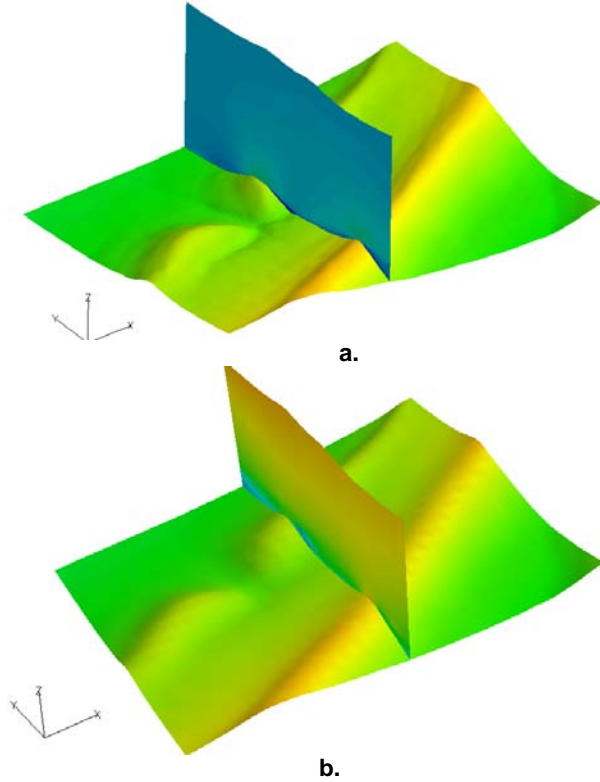


Figure 6. Comparison of velocity profiles perpendicular to the terrain for a) constant inflow velocity and b) inflow velocity specified from WRF 444 m input.

4.2 Internal Assimilation

We apply a Newtonian Relaxation data assimilation technique to incorporate the WRF data profiles into the CFD simulations. Such assimilation techniques are not common practice in CFD. The Acusolve code is modified to incorporate a body force that acts to “nudge” the modeled solutions toward an observation, in much the same way as is often done in NWP. For example, the body force appears in the u momentum equation as an additional forcing on the right hand side:

$$\rho \frac{\partial u}{\partial t} + \rho u \bullet \Delta u + \Delta p = \Delta \bullet \tau + \rho b . \quad (1)$$

Here u represents the x -velocity component, ρ is the density of the fluid, P is the pressure, τ is the surface and viscous stresses, and b is the incorporated body force:

$$b(x, y, z, t) = \frac{1}{\Delta t} (u_o - u_s) . \quad (2)$$

This body force depends on the innovation, that is, the difference between the observed velocity, u_o , and that simulated, u_s , modulated by the time step Δt . Figure 7 shows the impact of assimilation data from a notional meteorological tower within the CFD domain. The flow field without any assimilation appears in Figure 7a while 7b compares the same solution with assimilation via data from the tower. The impact of the assimilation on the downstream flow is apparent. The flow field has adjusted to the input, despite the fact that it is all imposed at a single grid profile for this demonstration. Note that we do not expect complete agreement because the terrain forcing of the CFD model will constrain the solution. One can see a vertical discontinuity in the profiles that is likely due to the data being assimilated at discrete vertical levels. This observation suggests that the spatial spreading function in Eq. (1), $W(\mathbf{x}, t)$, should include spreading the observation in the vertical direction as well. The fact that the upstream flow has additionally adjusted in strength assures us that AcuSolve is adjusting the entire flow field in a mass consistent manner.

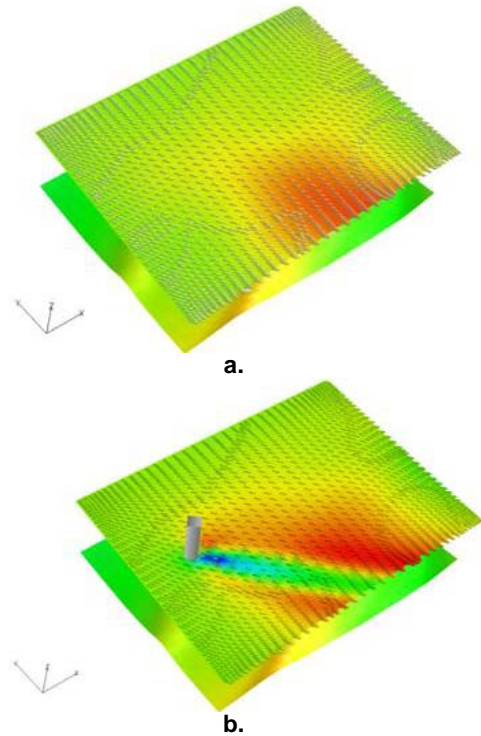


Figure 7. Flow field modified by the use of a notional body force. The top figure shows the flow field with no body force and the bottom one shows the corrected flow field.

Then we use a Cressman-type weighting function for the horizontal variation of $W(x,y,z,t)$ as is typically used in meteorology (Warner 2011), but it does not vary in time since the integration times are so small for the CFD simulation. Specifically, we allow a radial dropoff at a rate of $e^{-\frac{r}{2R}}$, where r is the radial distance from the observation point and R is arbitrarily set at 200 m for this initial study. This distance allows a smooth drop-off in influence over about four or five horizontal grid points yet avoids overlap in the areas of influence from two WRF grid points. Further study is needed to quantify the best approach for defining both G and W with respect to their influence on flow field quantities. Figure 8 contours the horizontal shape of the spreading function for the forcing that that is imposed on the flow at the two gridlines.

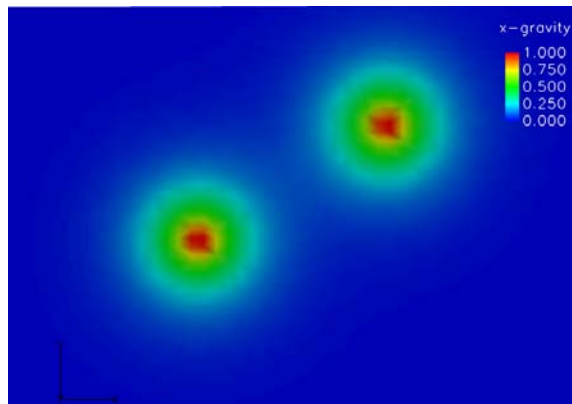


Figure 8. Cressman weighting functions for spreading the wind profiles.

5. RESULTS

The techniques described above were applied to the New Year's Eve 2008 case. The simulation included both the WRF inflow and the WRF point profile assimilation techniques.

First we wish to assess whether or not our CFD simulation can reproduce some relevant characteristics of the actual wind field. Unfortunately we were unable to obtain data from the two 10 m meteorological towers in the vicinity for the case day. We were, however, able to obtain a limited amount of data at a 2 m elevation measurement site just upwind of the saddle between the first set of parallel ridges. Note that when modeling a specific realization, we do not expect to exactly match the wind components due to ensemble variability. What we do hope to be able to match is the power density spectrum. Therefore, we compare the simulated with the

experimentally-derived power density spectra for both the u and v components of the wind at the measurement location in Figure 9. At low frequencies, the power densities compare quite well. At higher frequencies, the CFD curves show less power density than do the observational data. This result is expected and prevalent in most models. The drop-off in power density is due to over-dissipation, which is expected due to the effective model resolution being typically about seven times the actual resolution (Skamarock 2004). That same paper points out that some damping at the highest frequencies is prudent to avoid physically unrealistic structures. Therefore, the comparison in Figure 9 is quite reasonable.

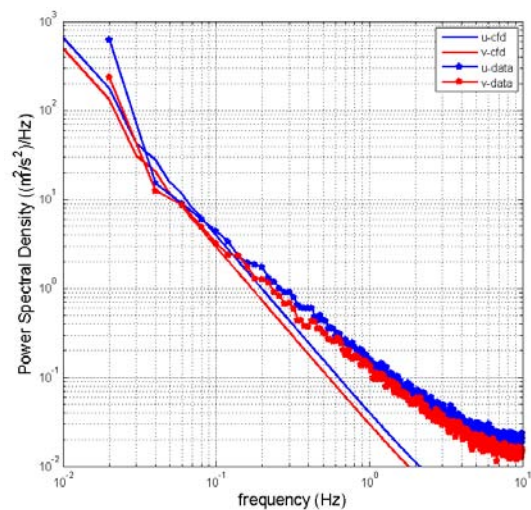


Figure 9. Comparison of spectra of wind components between the CFD simulation (solid lines) and observational data (stars) at 2m.

Figure 10 illustrates the preliminary results of data assimilation at the two sites chosen for study. The CFD without assimilation (green curves) represents the CFD simulation using WRF inflows only. The CFD with assimilation (red curves) signifies that both the WRF inflows were used and additional WRF profile data was assimilated at the given location. The original WRF data (black curves) refers to the WRF data at the grid point nearest to the location indicated. Note that the WRF data grid points are 444 m apart while the CFD grid is much finer. An exact match is not possible since two different grids are used. However, the WRF data does not vary substantially over the Rock Springs domain studied here, particularly in the valley. Our goal is to nudge the CFD solution from the CFD without assimilation toward the Original WRF data. Notice that the run with data assimilation nudges the profile closer to that of the WRF data at the Ag

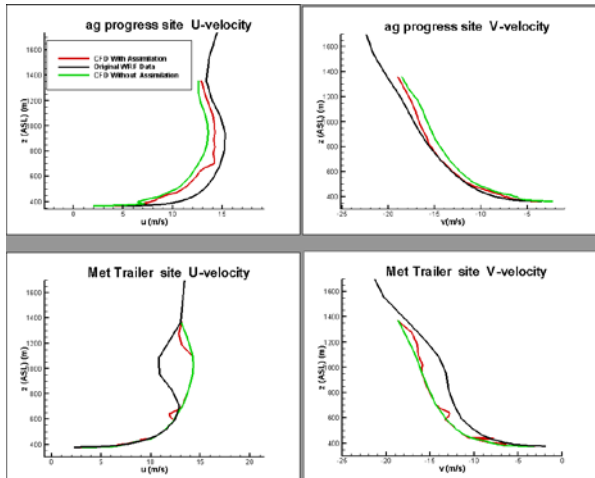


Figure 10. Preliminary results from assimilating WRF data at two internal points in the domain (CFD with Assimilation) in addition to only using the WRF data to specify the inflow (CFD with WRF Inflow).

Progress site. The met trailer site proved to be more difficult, however; the CFD with assimilation is modified somewhat from the CFD without assimilation run. Note that we do not expect complete agreement because the terrain forcing of the CFD model will constrain the solution. One can see a vertical discontinuity in the profiles that is likely due to the data being assimilated at discrete vertical levels. This observation suggests that the spatial spreading function in Eq. (8), $W(\mathbf{x},t)$, should include spreading the observation in the vertical direction as well.

Next we impose the Cressman radial weighting function. The results appear in Figure 11. Figure 11a shows streamlines for the case with no assimilation. These streamlines indicate smooth flow over the mountains and the underlying surface pressure field (colored) show the expected elevated pressure on the windward side of the ridge with a pressure minimum on the ridges. Figure 11b includes assimilation with the Cressman spreading as seen in the elevated pressure at the assimilation location. This pressure deviation is matched by complexity in the streamlines indicating that the flow is adjusting commensurately. Although we do not have field data for more detailed comparison, we are at least assured that the mass and momentum fields do respond to the imposed nudging. Further study is required to confirm that this adjustment improves the local flow solution. Together, these figures provide preliminary evidence that assimilating data into a high fidelity CFD simulation could be a feasible approach to combining information from the NWP mesoscale model into the fine scale CFD simulation.

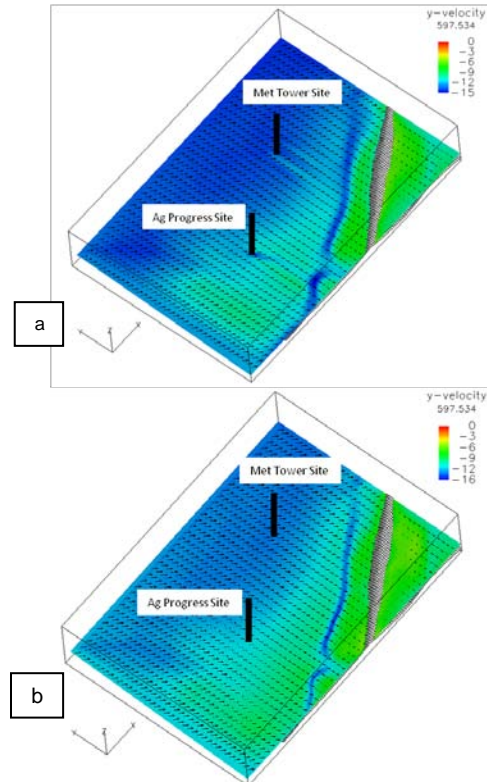


Figure 11. The effect of assimilating WRF data at two locations into the CFD solution. Panel b includes assimilation while panel a does not.

6. CONCLUSIONS AND PROSPECTS

This project has taken the first steps toward assimilating mesoscale model data into a CFD simulation. The assimilation uses both an inflow condition and a body force to incorporate interior wind profiles. Note that temporally varying conditions could also be used for dynamic assimilation.

This work incorporates WRF data into the CFD model in two ways: using the WRF data as inflow conditions for the CFD model and assimilating vertical profiles of the fine scale WRF data into the CFD model in order to nudge the CFD solution toward the WRF model data. Because WRF includes the outer boundary conditions from a global model, and the meteorological microphysics and radiation schemes to produce a solution that is contains the meteorological forcings, we hope to capture the synoptic details of the current particular situation. Thus, by doing such an assimilation, we expect to approach simulating a specific realization of fine scale atmospheric flow that indicates specific flow features and differential winds.

The preliminary results of this study indicate that incorporating the WRF data into the

AcuSolve simulation can nudge the wind profile towards that of WRF while retaining the mass consistency of the CFD model.

By using the spatially varying inflow and assimilating wind profiles from a fine-scale WRF run as forcing conditions for Acusolve, we can approximately replicate a realization for a particular time. Note that the WRF run used four dimensional data assimilation to produce a flow field consistent with simultaneous observations. The Acusolve computed wind field showed more variability in the flow field that did the constant velocity control run.

With further development the techniques investigated here could be useful in various contexts. In the wind energy industry, they could aid characterizing the specific inflow for an individual turbine site with respect to terrain and any nearby features, which is necessary for micrositing. Such information is also informative to nowcasting models, including statistical downscaling techniques. It could be explored as a technique for studying extreme and anomalous flow conditions that could lead to premature turbine failure (DOE 2008). This method could also be considered for modeling atmospheric transport and dispersion. Particularly for case analyses, the specific details of flow in this "terra incognita" region could prove advantageous. Finally, this technique could be of use in defining local flow features for assessing loads on manmade structures in the atmospheric boundary layer environment.

Acknowledgements: This research is supported by the Applied Research Laboratory of The Pennsylvania State University. We thank our colleagues in the Meteorology Department, specifically David Stauffer, Brian Gaudet, and Aijun Deng, for providing the mesoscale modeling data, which was produced under a contract to the Defense Threat Reduction Agency. The authors also thank ACUSIM Software, Inc. for supporting this work through licensing and technical assistance.

References

- ACUSIM Software, 2008: *AcuSolve Command Reference Manual*, Version 1.8, 462 pp.
- Beyer-Lout, A, 2007: *Concentration assimilation into wind field models for dispersion modeling*. Master's Thesis, The Pennsylvania State University, University Park, PA.
- Haupt, S.E., A. Beyer-Lout, K.J. Long, and G.S. Young, 2009: Assimilating Concentration Observations for Transport and Dispersion Modeling in a Meandering Wind Field, *Atmospheric Environment*, **43**, 1329-1338.
- Hoke, J.E., and R.A. Anthes, 1976: The Initialization of Numerical Models by a Dynamic Initialization Technique. *Mon. Wea. Rev.*, **104**, 1551-1556.
- Kalnay, Eugenia, 2003: *Atmospheric Modeling, Data Assimilation and Predictability*. Cambridge University Press, Cambridge, 136-204.
- Long, K.J., F.J. Zajackowski, S.E. Haupt, and L.J. Peltier, 2009: Modeling a Hypothetical Chlorine Release on a College Campus, *Journal of Computers*, **40**, 881-890.
- Lyons, D.C., L.J. Peltier., F.J. Zajackowski, and E.G. Paterson, 2009: Assessment of DES models for separated flow from a hump in a turbulent boundary layer. Submitted to *J Fluids Eng*.
- Skamarock, W.C., 2004: Evaluating mesoscale NWP models using kinetic energy spectra. *Mon. Wea. Rev.*, **132**, 3019-3032.
- Skamarock, W.C., J.B. Klemp, J. Dudhia, D.O. Gill, D.M. Barker, W. Wang and J.G. Powers, 2005: A description of the advanced research WRF version 2. NCAR Tech. Note NCAR/TN-468+STR, 88 pp.
- Stauffer, et al., 2008: FY08 Annual Report to the Defense Threat Reduction Agency for Sensitivity of Atmospheric Boundary-Layer Winds and Stability to Soil Moisture and Cloud Properties, Penn State University, 118 pp.
- Wilson, R.P., S.E. Haupt, and L.J. Peltier, 2009: Detached Eddy Simulation of Atmospheric Flow about a Surface Mounted Cube at High Reynolds Number, submitted to *J. Fluids Eng*.
- Warner, T. T., 2011, *Numerical Weather and Climate Prediction*, Cambridge University Press, 526 pp.